ISSN 1674-1056
http://cpb.iphy.ac.cn
http://iopscience.iop.org/cpb
中国物理 B
Chinese Physics
中国物理
Chinese Physics B

Direct simulation Monte Carlo study of metal evaporation with collimator in e-beam physical vapor deposition

Xiaoyong Lu(卢肖勇), Junjie Chai(柴俊杰)

Citation: Chin. Phys. B . 2019, 28(7): 074702. **doi:** 10.1088/1674-1056/28/7/074702
Journal homepage: http://cpb.iphy.ac.cn; http://iopscience.iop.org/cpb

What follows is a list of articles you may be interested in

Numerical simulation of metal evaporation based on the kinetic model equation and the direct simulation Monte Carlo method

Xiaoyong Lu(卢肖勇), Xiaozhang Zhang(张小章), Zhizhong Zhang(张志忠)
Chin. Phys. B . 2018, 27(12): 124702. **doi:** 10.1088/1674-1056/27/12/124702

A growth kinetics model of rate decomposition for $Si_{1-x}Ge_x$ alloy based on dimer theory

Dai Xian-Ying, Ji Yao, Hao Yue
Chin. Phys. B . 2014, 23(1): 015101. **doi:** 10.1088/1674-1056/23/1/015101

Transport properties of a binary mixture of CO_2–N_2 from the pair potential energy functions based on a semi-empirical inversion method

Song Bo,Wang Xiao-Po,Yang Fu-Xin,Liu Zhi-Gang
Chin. Phys. B . 2012, 21(4): 045101. **doi:** 10.1088/1674-1056/21/4/045101

Direct simulation Monte Carlo study of metal evaporation with collimator in e-beam physical vapor deposition

Xiaoyong Lu(卢肖勇)[1,2,†] and Junjie Chai(柴俊杰)[2]

[1] *Department of Engineering Physics, Tsinghua University, Beijing* 100084, *China*
[2] *Research Institute of Physics and Chemical Engineering of Nuclear Industry, Tianjin* 300180, *China*

(Received 11 January 2019; revised manuscript received 27 March 2019; published online 30 May 2019)

The flow properties and substrate deposition rate profile, which are the important parameters in electron beam physical vapor deposition, are investigated computationally in this article. Collimators are used to achieve the desired vapor beam and deposition rate profile in some applications. This increases the difficulty measuring boundary conditions and the size of the liquid metal pool inside the collimators. It is accordingly hard to obtain accurate results from numerical calculations. In this article, two-dimensional direct simulation Monte Carlo (DSMC) codes are executed to quantify the influence of uncertainties of boundary conditions and pool sizes. Then, three-dimensional DSMC simulations are established to simulate cerium and neodymium evaporation with the collimator. Experimental and computational results of substrate deposition rate profile are in excellent agreement at various evaporation rates and substrate heights. The results show that the DSMC method can assist in metal evaporation with a collimator.

Keywords: metal evaporation, collimator, deposition thickness profile

PACS: 47.45.–n, 51.10.+y **DOI:** 10.1088/1674-1056/28/7/074702

1. Introduction

Electron beam physical vapor deposition (EBPVD) plays an important role in many science and technology areas, such as thermal barrier coatings of turbine blades, the manufacturing of metal matrix composites, supersonic molecular beam technology, large-area corrosion protection coatings, and the enrichment of uranium.[1–3] In EBPVD, a high-energy electron beam is used to heat the metal ingot to create a molten metal pool, where the metal vapor expands from the surface to the vacuum. Collisions between vapor atoms continuously change their trajectories and velocities and then significantly influence their final position and substrate deposition rate, which is of critical importance. Fan *et al.* researched yttrium vapor deposition in a vacuum chamber both computationally and experimentally.[1] The atomic absorption spectra and deposition thickness profiles obtained by the direct simulation Monte Carlo (DSMC) method and experiments were in excellent agreement at two different evaporation rates. Venkattraman *et al.* carried out DSMC simulations to research the deposition of copper thin films by adding various molecular models for copper–copper interactions, and a suitable model was determined according to comparisons with published experimental data.[4] Moreover, the influences of thermal nonuniformities at the vapor source were discussed in another article.[5] Balakrishnan *et al.* investigated the influence of electronic excitation on the flow properties of titanium vapor, and the result compared with experiments showed that the electronic energy is an indispensable factor to consider in natural metal vapor flow.[2] Besides, Thakur and Sahu measured the spatial distribution of several metal vapors experimentally to match Knudsen's cosine law.[6–8] Chatain *et al.* measured the velocity, angular distribution, and population density of the ground and first four meta-stable states of gadolinium vapor by time-of-flight, deposition, and laser resonance absorption methods, respectively.[9]

In some applications of metal evaporation (e.g. the enrichment of uranium), a collimator is placed upon the crucible to achieve a desired divergence of the vapor beam and deposition rate profile. As a result, it is difficult to accurately monitor the temperature of the liquid metal pool surface because the collimator shelters it from optical sight.[10] Moreover, the collimator may be heated to make the metal that adheres to the inside walls of the collimator flow back into the crucible to improve the utilization ratio. This means that the sticking coefficient of metal vapor on the inside walls is not exactly 1 in the numerical calculation and experiments. In published papers, scientists usually concentrated on the domain upon the collimator by giving a specific incidence condition at the aperture and ignoring the rest of the domain.[11] However, although good agreements could be obtained at a certain correction, the practical significance of this method is relatively low.

In this article, we carry out DSMC simulations to calculate metal evaporation with a collimator in the whole domain. First, the problem is stated. Then several two-dimensional examples are calculated to quantify the influence of uncertainties of boundary conditions and pool sizes. Next, three-dimensional calculation results are compared with the experimental data of cerium and neodymium. Finally, some conclu-

[†]Corresponding author. E-mail: lu-xy15@mails.tsinghua.edu.cn

© 2019 Chinese Physical Society and IOP Publishing Ltd

sions are given.

2. Statement of the problem

A schematic diagram of metal evaporation with a collimator is shown in Fig. 1. Metal atoms that vaporize from the liquid metal pool surface are accelerated collisionally to the chamber surface. A fraction expands through the aperture of the collimator and then forms a vapor jet. Since the walls above the collimator are cold enough to completely freeze the metal atoms, the correct velocity distribution F and net mass flow rate M are obtained at the aperture, which are the only two principal influencing factors of flow properties above the collimator. This means that there is a right profile of deposition rate. The net mass flow rate M and velocity distribution F, which are functions of vapor source area S, vapor source temperature distribution $T_{\rm s}$, sticking coefficient α_i, and temperatures $T_{{\rm W}i}$ of the inside walls of the collimator, are given by Eqs. (1) and (2) as follows:

$$M = \Phi(S, T_{\rm s}, \alpha_i, T_{{\rm W}i}), \tag{1}$$

$$F = \Psi(S, T_{\rm s}, \alpha_i, T_{{\rm W}i}). \tag{2}$$

Unfortunately, the parameters in functions Φ and Ψ are difficult to measure accurately in experiments. As a result, a different calculation procedure based on the DSMC method is suggested to obtain the correct F and M. The procedure is described in detail in the next paragraph.

First, the surface of the liquid metal pool is divided into an isothermal high-temperature region and a low-temperature region. It is supposed that only the high-temperature region contributes to evaporation according to the formula for the saturated vapor pressure of metal. Then, an approximate area of the high-temperature region, which can be estimated according to the scan pattern of an electron gun, is presented. Next, we give the temperatures and sticking coefficients of the inside walls of the collimator. It is important to note that the values we present here are not necessarily actual. Finally, since the net mass flow rate M can be easily measured experimentally in metal evaporation with a collimator, the temperature of the high-temperature region is adjusted to match the flow rate M at the aperture. Numerical simulation results show that if the net mass flow rate is relatively low, the substrate deposition rate profile would be unrelated to the indeterminate quantities S, $T_{{\rm W}i}$, and α_i within a certain range, and so would the velocity distribution F at the aperture. There exists an accurate boundary condition corresponding to the actual boundary condition in a certain range because the boundary condition is presented rationally. Accordingly, the deposition rate profile obtained from calculations would be in good agreement with that obtained from experiments even though the quantities S, $T_{{\rm W}i}$, and α_i presented are inaccurate. This means that the deposition rate can be obtained by numerical calculations instead of experimental measurements if the net mass flow rate at the aperture and evaporation structure are known.

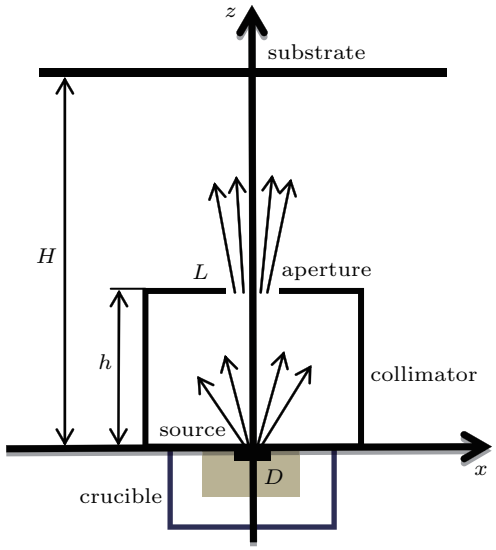


Fig. 1. Schematic diagram of metal evaporation with a collimator.

3. Results and discussions

Two-dimensional and three-dimensional DSMC simulations are carried out by employing the variable hard sphere (VHS) model. The collision cross section between two atoms has an inverse power relation with the relative speed in the VHS model. Furthermore, the scattering velocity after collision is isotropic in the center-of-mass system. The relationship between the collision cross section σ_T and the relative velocity $c_{\rm r}$ is given by

$$\sigma_T = \sigma_{T,{\rm ref}} \cdot (c_{\rm r,ref}/c_{\rm r})^{4/(\eta-1)}, \tag{3}$$

where $c_{\rm r,ref}$ denotes the reference relative velocity, $\sigma_{T,{\rm ref}}$ is the reference cross section at the reference temperature, and η is the coefficient of viscosity that originates from the experimental data. The values of alkali metal vapors have been measured experimentally and those of specific metals in this article are deduced from the literature.[1] Equation (4) gives the relationship between saturated vapor pressure P and temperature T of the metal pool surface.

$$\lg P = A/T + B \cdot \lg T + C. \tag{4}$$

Here, P denotes the saturated vapor pressure in the unit of mmHg, and A, B, and C are the fitting coefficients. The parameters of aluminum, cerium, and neodymium, the three metals in this article, are shown in Table 1.[12]

Table 1. Parameters of aluminum, cerium, and neodymium.

Metal	Aluminum	Cerium	Neodymium
$d_{\rm ref}$/Å	5.164	6.390	6.436
$T_{\rm ref}$/K	2000	2000	2000
η	7.351	6.531	6.531
m/u	26.98	140.1	144.2
$\lg P$/mmHg	$-16380/T - \lg T + 12.32$	$-20304/T + 8.207$	$-15299/T + 7.501$

An orthogonal coordinate system is employed in the simulation. A smaller cell size is adopted near the source surface and aperture to capture the rapid expansion of metal vapor, which is important for accurate calculations. About one million super particles are used. Particles arriving at the substrate are counted to obtain the deposition rate when the evaporation reaches stability.

Two-dimensional DSMC simulations at several net mass flow rates, the results of which are shown in Figs. 2–7, are carried out under various boundary conditions and widths of the liquid metal pool. The temperature of the aluminum pool surface is adjusted for the same net mass flow rate in each figure. Furthermore, two structures with different aperture widths (2 cm and 5 cm) are calculated for a wider applicability. The substrate is placed 30 cm above the aperture. The results show that both the boundary condition and the aluminum pool width have little influence on deposition rate at a low evaporation rate. Meanwhile, at a high evaporation rate (as shown in Fig. 4), it is obvious that profiles of substrate coating rates are quite different under several boundary conditions. As a result, the calculated coating rates are not credible at a high mass flow rate even though the profiles agree well in Fig. 7.

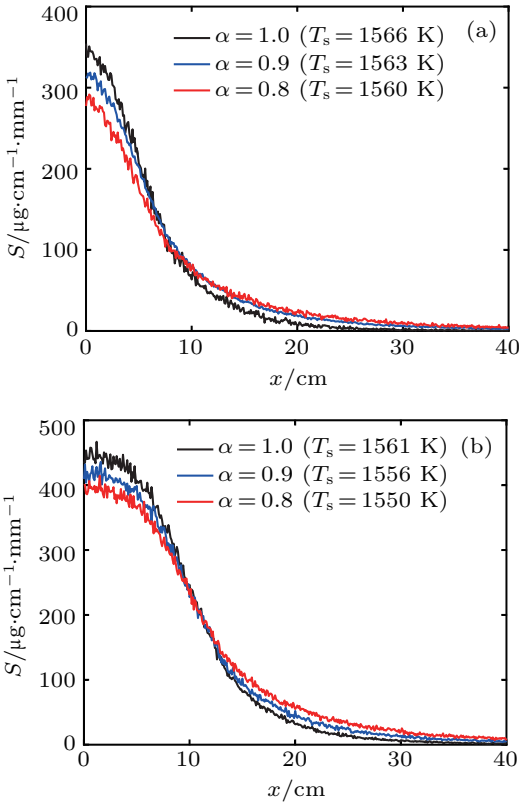


Fig. 3. Relationship between profile of deposition rates and boundary conditions at a moderate evaporation rate. (a) Narrow aperture (5.0 mg·cm^{-1}·min^{-1}); (b) wide aperture (10.0 mg·cm^{-1}·min^{-1}).

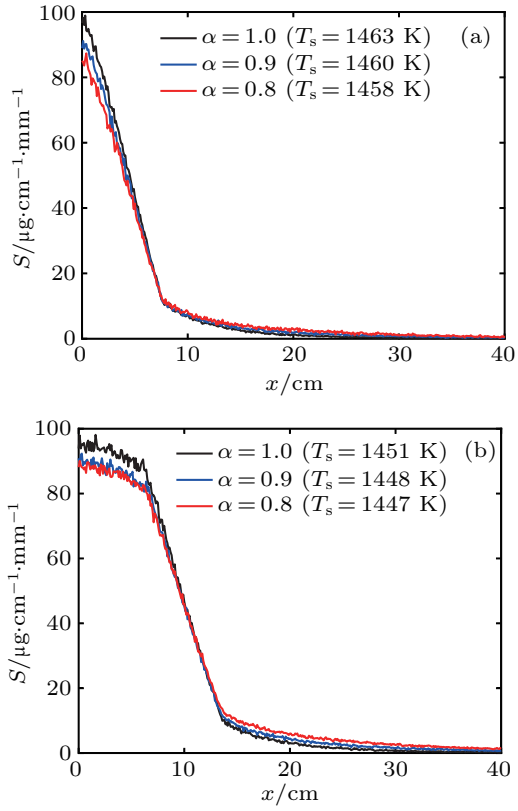


Fig. 2. Relationship between profile of deposition rates and boundary conditions at a low evaporation rate. (a) Narrow aperture (1.0 mg·cm^{-1}·min^{-1}); (b) wide aperture (2.0 mg·cm^{-1}·min^{-1}).

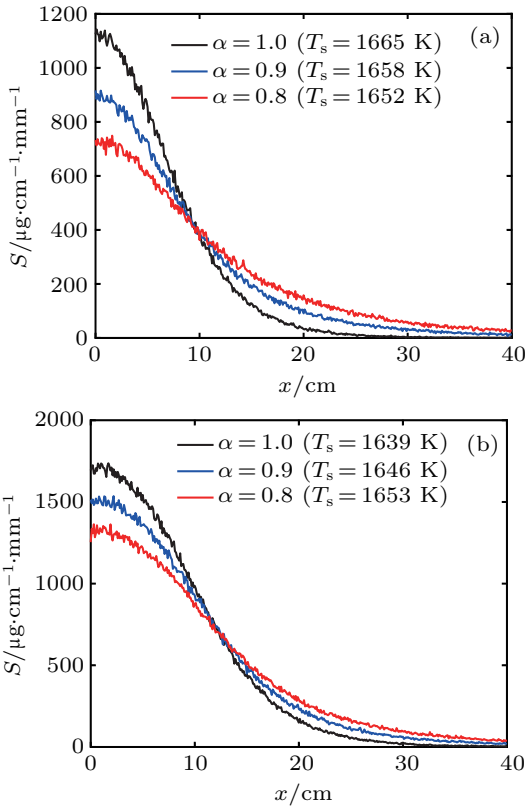


Fig. 4. Relationship between profile of deposition thickness and boundary conditions at a high evaporation rate. (a) Narrow aperture (20.0 mg·cm^{-1}·min^{-1}); (b) wide aperture (40.0 mg·cm^{-1}·min^{-1}).

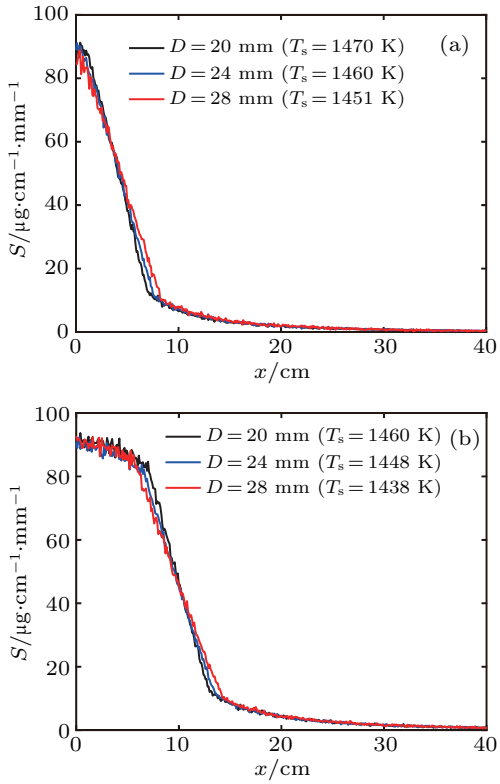


Fig. 5. Relationship between profile of deposition thickness and width of liquid metal pool at a low evaporation rate. (a) Narrow aperture (1.0 mg·cm^{-1}·min^{-1}); (b) wide aperture (2.0 mg·cm^{-1}·min^{-1}).

The numerical results can be explained as follows. Metal vapor atoms expand to the vacuum collisionally under ordinary circumstances. We suppose a limiting case of weak evaporation, in which the vapor flow above the liquid metal pool reaches the free-molecular or near free-molecular regime. As a result, it can be considered that vapor atoms at the aperture come from only two parts. The vast majority fly from the pool surface directly without any collision while the rest initially collide with the inside wall of the collimator once (the tiny minority of atoms that undergo several collisions is ignored). The profiles of substrate deposition rate shown in Fig. 2 can be divided into two parts: the body mainly coming from the vast majority mentioned above, and the wings consisting of the atoms with collisions. The boundary conditions have little influence on the profile because few atoms that deposit have experienced collisions. It is appropriate at a low evaporation rate for small proportion of wings though the thickness of wings are relatively impressible. However, metal atoms collide with each other more and more frequently with the increase of evaporation rate. Meanwhile, frequent collisions of atoms against boundary make themselves rebound back and the velocity distribution of vapor inside the collimator is influenced by the boundary condition, so is that at the aperture. As a result, the wings account for a considerable proportion of the profiles. This means that the body is quite different from the wings because the evaporation rates in Fig. 4 are the same. The variation tendencies are revealed clearly in Figs. 2, 3, and 4. Besides, the width of the liquid metal pool only affects the distribution of mass flux close to

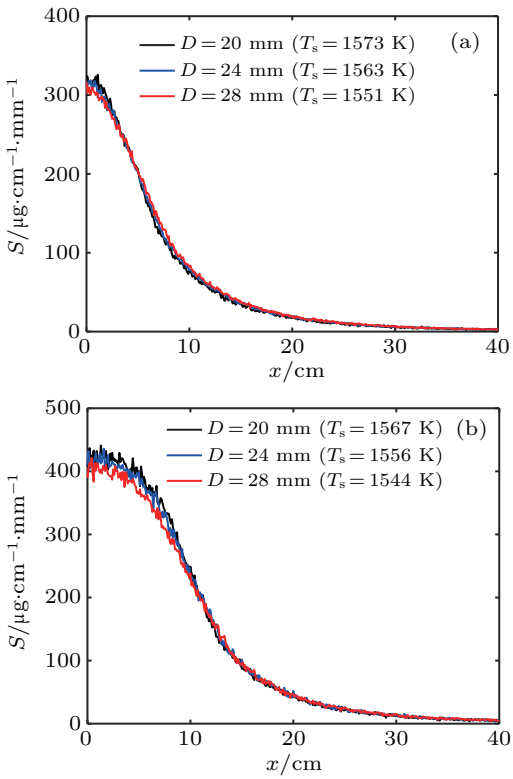


Fig. 6. Relationship between the profile of deposition thickness and the width of the liquid metal pool at a moderate evaporation rate. (a) Narrow aperture (5.0 mg·cm^{-1}·min^{-1}); (b) wide aperture (10.0 mg·cm^{-1}·min^{-1}).

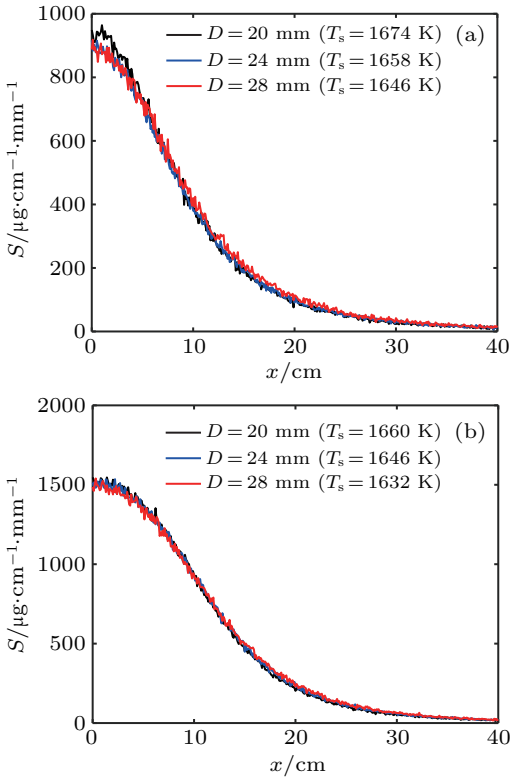


Fig. 7. Relationship between the profile of deposition thickness and the width of the liquid metal pool at a high evaporation rate. (a) Narrow aperture (20.0 mg·cm^{-1}·min^{-1}); (b) wide aperture (40.0 mg·cm^{-1}·min^{-1}).

the pool surface since the evaporation rate at the aperture stays the same in Figs. 5, 6, and 7. The difference in mass flux distribution is smoothed in the wake of vapor expansion, especially at a high evaporation rate. Therefore, the negligible influence of pool width can be ignored.

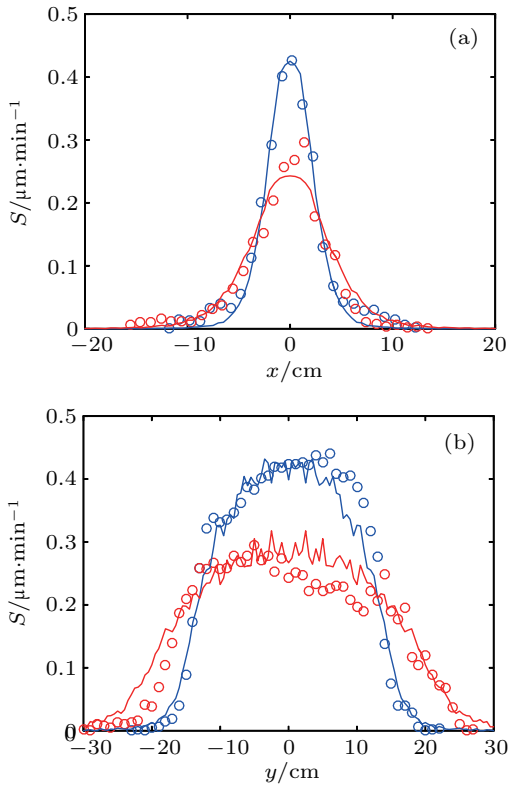


Fig. 8. Comparison of DSMC and cerium experimental deposition thickness profiles. The lines represent DSMC and the circles represent experimental data; the blue color indicates 50 cm and the red color indicates 70 cm. (a) Length direction; (b) width direction.

Figure 8 shows comparisons of the substrate deposition rates obtained by three-dimensional DSMC simulations and measurements of a film thickness gauge. The experimental arrangements are similar to those in Fig. 1. A 30 cm-high cuboid collimator is set on the crucible; on the upper surface of the collimator, a 2 cm×16 cm rectangular aperture is carved. The niobium substrate is centrally mounted above the crucible at heights of 50 cm and 70 cm to measure the profiles of deposition thickness. Other auxiliary and nonessential devices are not introduced in detail. DSMC simulations are carried out according to the specific experimental structure and net mass flow rate. A quarter volume of the domain is calculated for the symmetry of the structure, and the rest is mirrored. The net mass flow rate of cerium at the aperture in the experiment is about 70 mg/min–80 mg/min, and temperature of the pool surface is adjusted to match the mass flux in the numerical calculation. The mass deposition rate at the center point of the substrate in calculations are modulated to be equivalent to the film coating rate in experiments in Fig. 8 because the film density is not clear.[13] The deposition rates along two symmetric axes show excellent agreement. It is noted that experimental data are not symmetrical because the scan of the electron gun is not ideal.

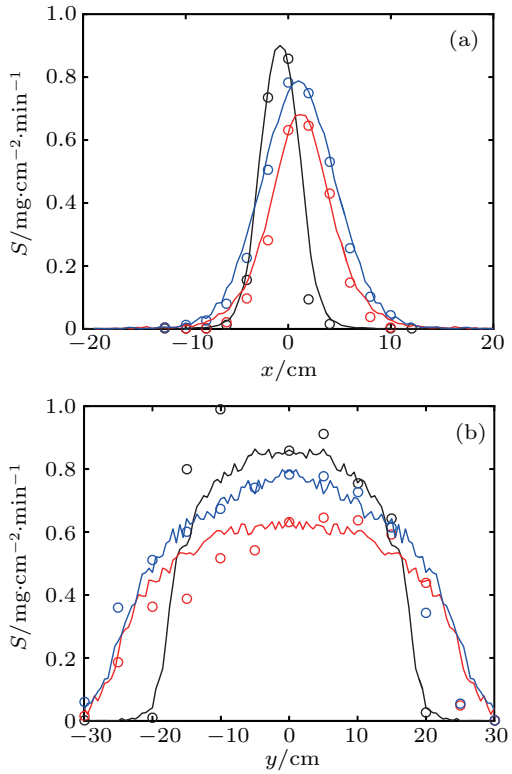


Fig. 9. Comparison of DSMC and neodymium experimental deposition rate profiles. The lines represent DSMC and the circles represent experimental data; the black color indicates 50 cm and 142 mg/min, the red color indicates 70 cm and 183 mg/min, and the blue color indicates 70 cm and 266 mg/min. (a) Length direction; (b) width direction.

A similar structure with a 2 cm×20 cm aperture is used for neodymium evaporation, and the corresponding DSMC simulations are carried out. The deposition weights are measured by weighing the mass changes of patches before and after the experiment at the evaporation rates of 142 mg/min, 183 mg/min, and 266 mg/min, respectively. The deposition rates shown in Fig. 9 are the deposition weights divided by patch area. It can be easily seen that experimental data have obvious fluctuations along the y-axis in Fig. 9(b). Besides, some negative experimental numbers measured at the edge of the substrate are not displayed in the figures. The fluctuations are caused by film abscission and oxidation when the vacuum chamber is opened. Profiles of simulations in Fig. 9(a) are translated along the x-direction to match the experimental data for asymmetry because the scan of the electron gun is not always symmetrical in experiments. The results in the length direction and width direction are in good agreement.

4. Conclusion

Metal evaporation with a collimator is investigated by the DSMC method. First, some uncertainties of boundary conditions and the size of the liquid metal pool in the simulation

are introduced. Then, two-dimensional DSMC calculations are carried out, verifying that the uncertainties have little influence at a low evaporation rate. Finally, three-dimensional DSMC calculations for cerium and neodymium evaporation are performed, and the numerical profiles of deposition rates are compared with those measured by a film thickness gauge and weighting. The results show quantitative agreement under different metals, evaporation rates, and substrate heights. Therefore, it is reasonable to adopt the DSMC method to study metal evaporation with a collimator. It is almost certain that the simulation would be useful for subsequent experiments.

Acknowledgment

The authors would like to thank our colleague Dr Xuming Lv for supporting the experimental data.

References

[1] Fan J, Boyd I D and Shelton C 2000 *J. Vac. Sci. Technol. A* **18** 2937
[2] Balakrishnan J, Boyd I D and Braun D G 2000 *J. Vac. Sci. Technol. A* **18** 907
[3] Rossnagel S M 2003 *J. Vac. Sci. Technol. A* **21** S74
[4] Venkattraman A and Alexeenko A A 2010 *J. Vac. Sci. Technol. A* **28** 916
[5] Venkattraman A and Alexeenko A A 2011 *J. Vac. Sci. Technol. A* **29** 041509
[6] Thakur K B and Sahu G K 2002 *J. Phys. D: Appl. Phys.* **35** 1812
[7] Thakur K B and Sahu G K 2004 *Vacuum* **75** 283
[8] Thakur K B and Sahu G K 2006 *Vacuum* **81** 77
[9] Chatain S, Gonella C and Roblin P 1997 *J. Phys. D: Appl. Phys.* **30** 360
[10] Dikshit B, Zende G R, Bhatia M S and Suri B M 2008 *Meas. Sci. Technol.* **19** 025103
[11] Venkattraman A and Alexeenko A A 2012 *Vacuum* **86** 1748
[12] Iida T and Guthrie R I L 1988 *The Physical Properties of Liquid Metals* (Translated by Xian A P and Wang L W) (Beijing: Science Press) pp. 91–92 (in Chinese)
[13] Chaleix D, Choquet P, Bessaudou A, Frugier L and Machet J 1996 *J. Phys. D: Appl. Phys.* **29** 218